Volume 18
Number 6
14 February 2022
Pages 1103–1332

Soft Matter

rsc.li/soft-matter-journal

ISSN 1744-6848

ROYAL SOCIETY OF CHEMISTRY

PAPER
Anton Peshkov *et al.*
Synchronized oscillations in swarms of nematode *Turbatrix aceti*

Soft Matter

ROYAL SOCIETY OF CHEMISTRY

PAPER

View Article Online
View Journal | View Issue

Cite this: *Soft Matter*, 2022, **18**, 1174

Synchronized oscillations in swarms of nematode *Turbatrix aceti*†

Anton Peshkov, * Sonia McGaffigan and Alice C. Quillen

Received 2nd November 2021,
Accepted 6th January 2022

DOI: 10.1039/d1sm01572a

rsc.li/soft-matter-journal

There is a recent surge of interest in the behavior of active particles that can at the same time align their direction of movement and synchronize their oscillations, known as *swarmalators*. While theoretical and numerical models of such systems are now abundant, no real-life examples have been shown to date. We present an experimental investigation of the collective motion of the nematode *Turbatrix aceti* that self-propel by body undulation. We discover that these nematodes can synchronize their body oscillations, forming striking traveling metachronal waves, which produces strong fluid flows. We uncover that the location and strength of this collective state can be controlled through the shape of the confining structure; in our case the contact angle of a droplet. This opens a way for producing controlled work such as on-demand flows or displacement of objects. We illustrate this by showing that the force generated by this state is sufficient to change the physics of evaporation of fluid droplets, by counteracting the surface-tension force, which allow us to estimate its strength. The relatively large size and ease of culture make *Turbatrix aceti* a promising model organism for experimental investigation of swarming and oscillating active matter capable of producing controllable work.

Introduction

Collections of biological organisms can be considered active materials[1] as energy is continuously dispersed through their motion. Two kinds of collective behavior can be distinguished for such organisms. On one hand, the self-propulsion of the organisms can lead to collectively moving states such as "turbulence" in bacterial suspensions,[2] flocking of birds[3] or schools of fishes.[4] On the other hand, some organisms performing periodic actions can synchronize their oscillations, such as the synchronous flashing of bugs,[5] crowd synchrony of pedestrians walking on a bridge[6] or flagella of microorganisms that beat in phase with one another.[7] The latter example is particularly interesting as it can lead not only to "in-phase" synchronization but also to "moving phase" or traveling motion known as metachronal waves.[8–10]

A model that combines these two types of collective motion into particles that at the same time self-propel and synchronize their oscillations have recently been proposed in the form of swarmalators studied in ref. 11. In this model, the position of the particles and the state of the oscillator are interdependent, which distinguish it from previous studies where these two quantities were assumed to be independent. This model has since been complemented by more analytical and numerical investigations,[12–15] which found states with locally synchronized oscillations and particles traveling in waves. However, none of these studied models have shown a traveling wave state. A possible experimental realization of swarmalators has been proposed and numerically studied in ref. 16 in the form of undulating synthetic active flexible sheets, reminiscent of our nematodes. However, no experimental realization of collectively moving and oscillating particles has been demonstrated until this time.

In this study we report on collective behavior in a system of undulating nematodes *Turbatrix aceti* (*T. aceti*) commonly known as vinegar eels. The vinegar eels are widely used in aquaculture as food for young fishes and crustaceans. Therefore, they can be easily sourced from aquarium supplies stores and their culture methods are straightforward. The nematodes need to undulate to self-propel, and as we show in this paper, the synchronization of these oscillations leads to the formation of a collective metachronal wave. While these waves are similar to the one observed in cilia, the vinegar eels are not affixed to the wall, and can exit and enter the wave which slowly moves along the border. We presented a possible theoretical description of the synchronization of oscillations in ref. 17, this article present the experimental results.

The collective behavior of mobile particles can be sensitive to the number of spatial dimensions in which they evolve,[18,19] as well as to confinement and container geometry due to interactions with a boundary.[20–23] We show that the formation

Department of Physics and Astronomy, University of Rochester, Rochester, NY 14627, USA. E-mail: apeshkov@ur.rochester.edu

† Electronic supplementary information (ESI) available. See DOI: 10.1039/d1sm01572a

of the metachronal wave by *T. aceti* in a three-dimensional space is induced by confinement, in our case that of a contact angle of the droplet in which they swim. The confinement geometry not only controls the location of the collective state, but also the number of nematodes involved in collective beating and therefore the strength of the produced flow.

Past experimental investigation using bacterial suspensions have been able to displace objects,[24,25] extract energy[26] or produce controlled organized flows.[27] However, extraction of energy and flow productions has only been achieved by trapping individual bacteria in special cells and using their outside sticking flagella as motors.[26,27] While cilia are well known to produce fluid flows, they are attached to the surface, and external control has only been achieved for synthetic variants.[28] We show that the force produced by the collective motion of *T. aceti* is substantial and sufficient to change the evaporation mode of a droplet in which they swim. This let us anticipate the possibility of designing channels with controlled flows as well as objects pushed by the nematodes.

Characterization of the collective state

We grow and study *T. aceti* in a 1 : 1 solution of water and apple cider vinegar. To investigate the collective motion, we put droplets of high density solution of nematodes ($d \geq 10$ n μl^{-1}) on glass slides whose surface was treated with a hydrophobic PDMS compound. Most experiments were done with 100 μl droplets, though we verified that similar behavior can be observed in droplets up to 1000 μl and down to 50 μl. Additional information on the preparation and experiments is available in the ESI,† SII.

Initially the motion of nematodes in the droplet is random as can be seen in Fig. 1(a) and movie SM1 (ESI†) (movies are available at ref. 29). After the deposition on glass, the nematodes start to concentrate on the border of the drop due to bordertaxis.[30] Individual nematodes that approach the border continue moving along the border as expected for active particles. After a variable period of time, depending on the droplet volume and evaporation conditions, the oscillation of groups of nematodes on the border becomes locally synchronized. If the concentration of nematodes in the initial droplet is large enough, with number of organisms per unit volume $d_{wave} \gtrsim$ 10–20 n μl^{-1}, the locally synchronized swarms will grow in size until finally percolating into a metachronal wave that spans the whole border of the droplet, as represented on Fig. 1(b) and movie SM2 (ESI†). The number of nematodes participating in the wave and the degree of synchronization increase in time until reaching a maximum wave strength as illustrated in

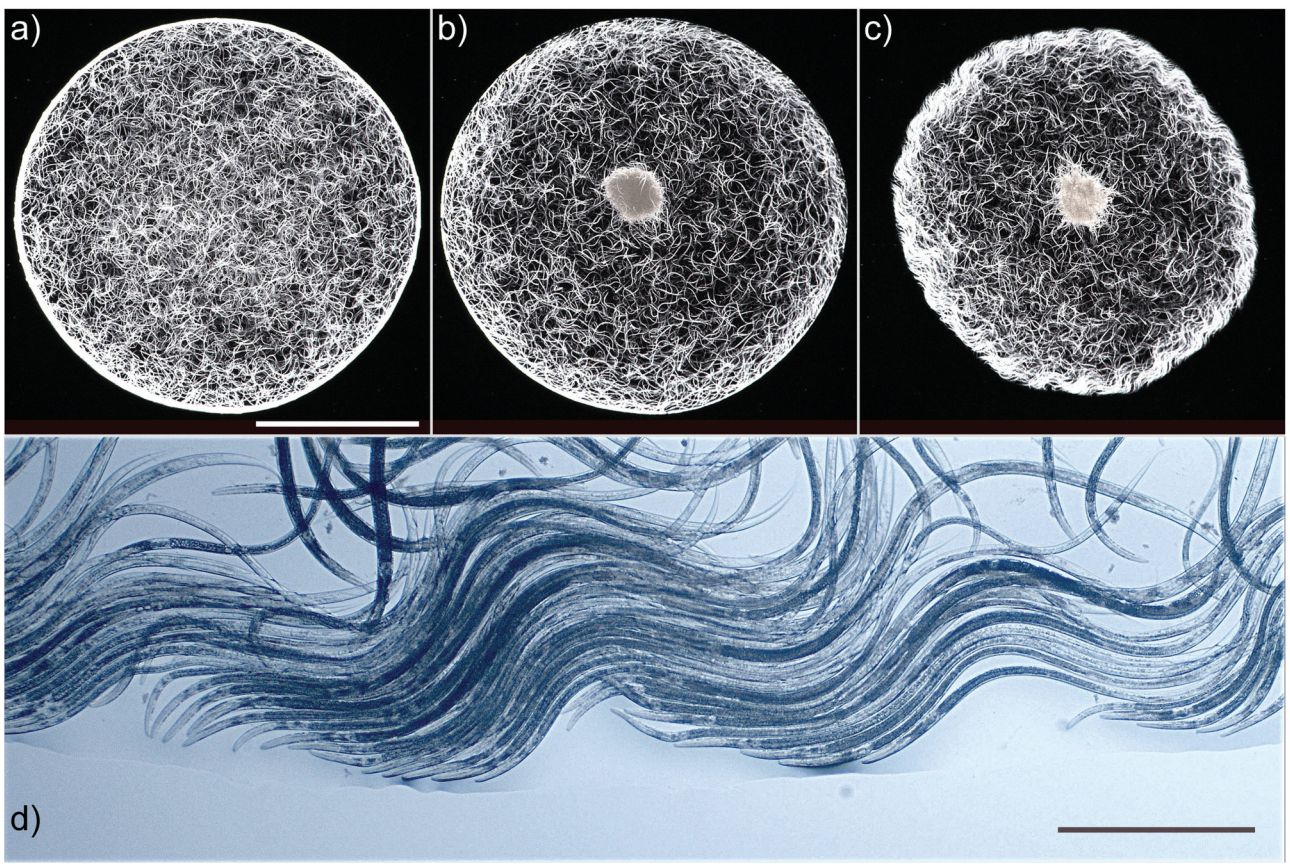

Fig. 1 Top: (a–c) Photos of evaporation of a 250 μl droplet at different moments in time. Initial density of nematodes in the droplet was $d = 30.7 \pm 3.3$ n μl^{-1}. Scale bar is 5 mm. (a) $t = 1$ min, random motion. (b) $t = 20$ min, percolation of the metachronal wave at the border. (c) $t = 60$ min, fully developed metachronal wave. (d) A view of the metachronal wave similar to that in (c) under a microscope with 4× magnification. Scale bar is 0.5 mm.

Fig. 1(c) and movie SM3 (ESI†). To the best of our knowledge, this is the first report of such collective motion in this, or any other specie of nematodes. The existence of this, both swarming and oscillating, state is the first major finding of this manuscript.

Observing this collective wave under a microscope (Fig. 1 and movie SM4, ESI†), we can see that the nematodes orient their head toward the border and synchronously oscillate at an angle from 0 to 90°. While nematodes of different ages and sizes are present in the solution, only similarly sized adult ones participate in the wave. Smaller nematodes are expelled to the center of the drop. We were able to observe wave frequencies f_{wave} in the range of 4–8 Hz, consistent with that of individual nematodes. Though the majority of experiments produced waves with lower frequencies in the 4–5 Hz range. While the mechanism of selection of beating frequency needs to be elucidated, once the wave is formed, the frequency remains constant for the lifetime of the wave. In addition to their oscillations, the nematodes slowly move along the border with a typical velocity of $v_{\mathrm{border}} \approx 0.1$ mm s^{-1}. This velocity is lower than that of freely swimming nematodes $v_{\mathrm{swim}} \approx 0.4$ mm s^{-1} and an order of magnitude smaller than the velocity of the phase of the metachronal wave $v_{\mathrm{wave}} \approx 46$ mm s^{-1}. Note that in this state, the position and the velocity of the nematodes is controlled by the oscillations of the nearby nematodes. In that sense, this state is a realization of *swarmalotors*.

In more than 70% of the experiments that we have performed, the wave rotates in the counter-clockwise direction. We do not have an explanation for this symmetry breaking. A similar symmetry breakage was observed in colonies of rotating magnetotactic bacteria under the influence of a magnetic field.[31] It was speculated that this absence of symmetry could be due to the helicity of the bacteria. Therefore, this skewness of rotational direction of the wave that we observe could indicate a possible asymmetry in the motion of individual swimming nematodes, though we were not able to observe it in practice.[17]

In addition to the metachronal wave, we often observe the formation of a compact cluster of nematodes in the vicinity of the center of the droplet and a strong reduction in the density of nematodes in the space between the border and the dense cluster at the center (see Fig. 1(b) and (c)). When observed under the microscope, the cluster presents itself as a knot of highly entangled nematodes similar to the ones recently observed for *C. elegans* on solid surfaces[32] as well as *T. tubifex*[33] and *L. variegatus*[34] in liquid. This cluster is not stable in time and can grow and shrink during the experiment. The dynamics of these clusters is out of the scope of this article and will be presented in future works.

When the wave is formed, it is generally stable until the end of its life. However, instabilities can be observed for large droplet sizes (>500 μl) and in droplets with low contact angles ($<30°$). A temporal increase in size of the central cluster can lead to the depletion of nematodes at the border and the disappearance of the wave. More information on instabilities is provided in part IV (ESI†).

If the contact angle of the drop is low enough, a strong deformation of the border of the drop will occur, as can be seen in the movie SM5 (ESI†). This deformation of the border stems from the motion of the bodies of the nematodes as we argue in the following section. The ondulatory motion of nematodes body also produce strong fluid flows. Indeed we were often able to observe a rotational motion of the free swimming and clustered nematodes, which were not part of the wave, as well as of tracer particles, in the center of the droplet, as illustrated by the movie SM6 (ESI†). In the mentioned movie, we measured the rotational velocity in the center of the drop to be around 1.3 rpm. Given that the fixed quantity is the above-mentioned metachronal wave travel velocity v_{wave}, the rotational velocity will decrease in larger droplets and will increase in smaller ones.

Conditions for the collective state

We are interested in identifying parameters that control the appearance of the metachronal wave during the evaporation of the droplet. One hypothesis would be that the metachronal wave appears when the density of nematodes reaches a threshold value. However, as mentioned before, we see the appearance of metachronal wave for all the droplets as soon as the initial concentration of nematodes is sufficiently large 10–20 n μl^{-1}. Neither the time, nor the size of the droplet is a determining factor as we show below. We have discovered that the control parameter for the formation of the metachronal wave is the drop contact angle.

Fig. 2(a) shows the contact angle of several selected droplets as a function of time. We selected several representative droplets of different densities, volumes, initial contact angles and evaporation rates. We indicate with a vertical bar, on each curve, the time at which the metachronal wave spanning the whole drop perimeter appears. We can see that time is not a determinant parameter for the formation of the collective state, with times ranging from several seconds to several hours. However, the metachronal wave appears for all the droplets at approximately the same contact angle. We have measured the critical angle for the percolation of the metachronal wave to be $\theta_c = 68.5 \pm 1°$.

This phase transition to the collective state at a particular angle is confirmed by analyzing the number of oscillating nematodes at the border of the droplet d_b (Fig. 2b). For droplet contact angles superior to θ_c, the density of nematodes at the border is mostly independent of the angle and is directly proportional to the density of nematodes in the initial solution (Fig. 2c). However, past the critical angle the density of nematodes start to increase. In the case of an initial density insufficient to form a full wave, we see only a small increase in density up to an angle of around 60°, and staying constant afterwards. In contrast, for droplets in which a collective wave appears, the density at the border grows until reaching a maximum at an angle close to 35°. The maximum density at the border seems to be independent of the initial concentration of the solution. This can be easily explained, as the maximum

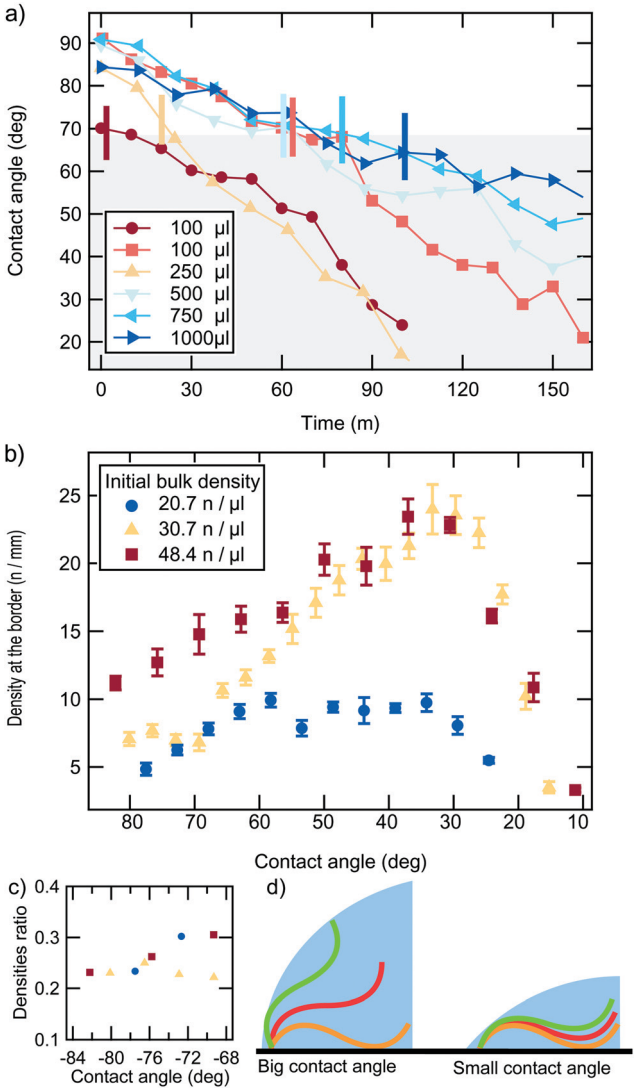

Fig. 2 (a) Contact angle of evaporating droplets over time. Different lines represent different experiments with different initial volumes and concentrations, as well as different evaporation conditions. The 250 µl droplet is the same as Fig. 1(a)–(c). Colored vertical lines represent the approximate time when the full drop spanning metachronal wave was formed. The shadowed gray area corresponds to the angles $<68.5^\circ$ where the metachronal wave exists. The estimated standard deviation on angle determination is 4°. (b) Density of nematodes at the border as a function of the contact angle for three different initial density of nematodes in the solution. No metachronal wave was observed for the lowest density. Error bars are standard mean error. (c) Ratio of border to bulk density for contact angles superior to θ_c. (d) A possible explanation of the dependence of the collective state on the droplet contact angle. At high contact angle (left), the nematodes are unlikely to touch each other. At low contact angle (right), the nematodes will touch each other and therefore synchronize their motion.

instantaneous density that we were able to observe was 29.9 n mm^{-1}. Given that the typical width of a single nematode participating in the wave is 29(5) µm, this allows us to estimate the densest "close-packing" at 34.5(6.0) n mm^{-1}, for nematodes perpendicular to the surface. However the nematodes bodies are oscillating at a tilt of $\sim 20^\circ$,[17] which limits the maximum density to $\sim$32.4 n mm^{-1}, slightly higher than the value we measured. For droplet contact angles inferior to 30°, we observe a sharp decrease in the number of the nematodes on the border and a disappearance of the collective wave. This can be explained by the space constraint which does not allow the nematodes to effectively fit into the fluid volume near the border. The dependence of the location and strength of the metachronal wave on the contact angle of the droplet is the second major finding of this manuscript.

A natural question is why the formation of the wave would depend on the contact angle. Our hypothesis is represented in Fig. 2(d). In ref. 17 we suggested that the synchronization of nematodes is facilitated by steric interactions between them. If the contact angle of the droplet is high, the probability that two nematodes oscillating at the border and located nearby one another will touch is relatively low, as they will in most cases oscillate at different angles to the surface, making synchronization less likely. In the opposite case, if the contact angle of the droplet is low and the drop is very shallow, two nematodes oscillating nearby will almost certainly touch each other and strongly interact and synchronize their motion. Note that the synchronization of the motion of nematodes, will "free-up" the space at the border, as they can be closer to one another. This explains the increase in concentration near the border as the angle of the droplet decrease, and the wave becomes more synchronized. It is also important to remark that, the concentration of nematodes at the border is dependent on the contact angle, but not the "history" of achieving this angle as illustrated by the droplet that started at an angle of 70° on Fig. 2(a). Thus the bordertaxis is not due to any outward flows due to droplet evaporation like in the "coffee-ring" effect, as opposed to for example the motion of microalgae Chlamydomonas reinhardtii inside droplets.[35]

Droplet evaporation

The physics of drop evaporation is relatively complex and depends on the properties of the liquid, the surrounding gas and the surface on which the drop resides.[36] The process of drop evaporation is generally divided into two or three main stages.[37] In the following we will focus on the first stage of evaporation, neglecting the later stages of very sharp reduction in the droplets contact angle or diameter. There exist two different modes[38] of this phase of drop evaporation as shown in Fig. 3(a). The first, and most common case, notably for water on glass, is a constant contact surface area, when the drop evaporates through the decrease of the contact angle. For simplicity we will refer to this mode as the one at a constant diameter, as diameter is the parameter that we measure. This mode of evaporation will appear if the wetting contact forces to the surface are greater than the surface tension forces. For most common fluids, such as water, the initial contact angle of the drop will be less than 90°.[39] However, on some hydrophobic surfaces, the wetting force will be less than the surface tension force. In that second case, the drop will reduce its surface area

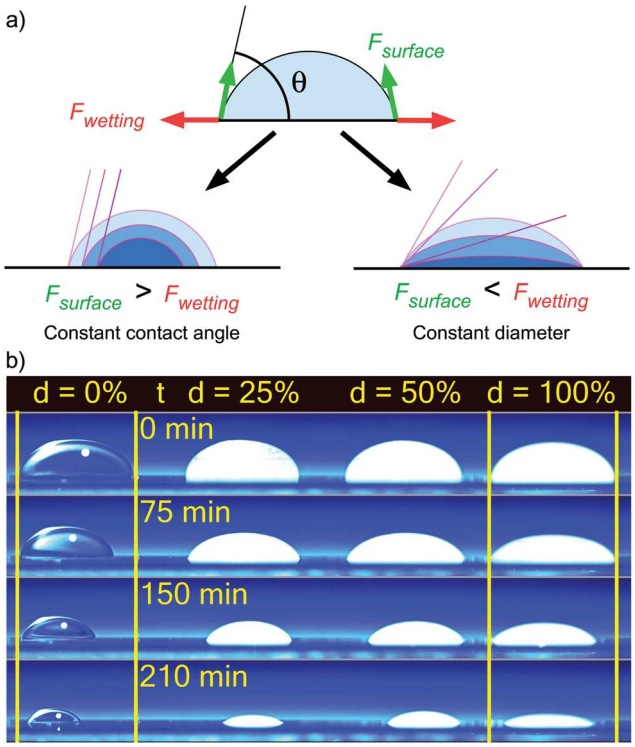

Fig. 3 (a) Diagram of two different possible modes of drop evaporation depending on the force balance between the fluid and the surface. (b) Side view of four 100 μl droplets with different nematode concentrations during evaporation. The concentrations of nematodes are from left to right 0%, 25%, 50%, 100%, with the rightmost drop with a density of d = 90.2 n μl^{-1} taken as a reference. Vertical yellow lines show initial borders of the 0% and 100% concentration droplets.

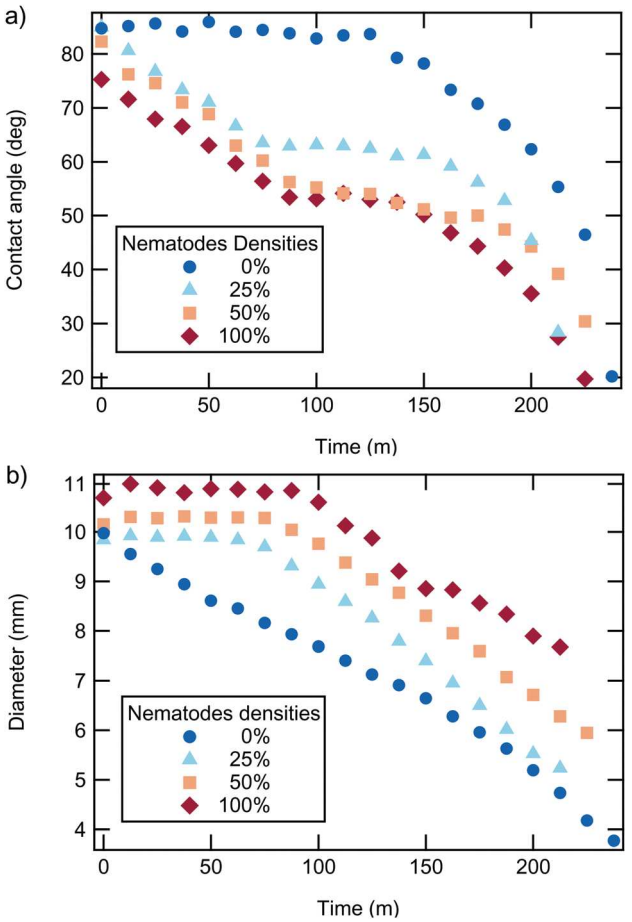

Fig. 4 Contact angles (a) and diameters (b) of the droplets from Fig. 3 as a function of time. The estimated standard deviation is 1° for the angle and 0.1 mm for the diameter.

while maintaining a constant contact angle during evaporation, and the drop diameter will decrease. Examples of such surfaces for water are polytetrafluoroethylene (PTFE, commonly known as Teflon) and the PDMS that coat our glass slides.[39] For most fluids, including water, the initial contact angle on such surface will be typically equal or greater than 90°.[39]

Since our slides were covered with hydrophobic PDMS, we will expect the contact angle to remain constant during evaporation. However we have seen in the previous section that this was actually not the case for our droplets with the nematodes. To confirm these, we perform an experiment with four droplets of different concentrations, prepared from the same initial dense solution. Because vinegar and other suspended particles in the grow solution will inevitably affect the droplet evaporation, for this experiment we transfer the nematodes into distilled water as described in the Methods section. While such a transfer present a risk of nematodes swallowing and busting due to osmosis,[40] we have not observed a change of their behavior in the short time span of up to four hours of these experiments.

Fig. 3(b) shows the side view of four droplets at different moments of time for four different concentrations of nematodes: 0%, 25% (d = 22.5 n μl^{-1}), 50% (d = 45.1 n μl^{-1}) and 100% (d = 90.2 ± 5.3 n μl^{-1}). As expected for water, the 0% density droplet evaporates by reducing the diameter. On the contrary, the droplets with the nematodes initially evaporates with a constant diameter and decreasing angle. Fig. 4 shows the extracted contact angles and diameters of these droplets. The d = 0% droplet evaporates with a constant contact angle and a continuously decreasing diameter until reaching the second phase of evaporation when the contact angle starts to rapidly decrease. For the droplets with the nematodes, we observe a reduction in contact angle until it reaches a transition angle θ_t, which is different for each droplet. After reaching θ_t, the droplets transition from the constant diameter mode of evaporation to the constant contact angle mode. Finally, at even later times, the second stage of evaporation with a sharp decrease in contact angle is observed. Surprisingly, the diameter of the droplets with the nematodes slightly increase at the beginning, an observation made by us in many experiments. This maybe explained by the facilitation of the contact point hysteresis by the random motion of the nematodes near the border. That the collective motion of nematodes can affect the physics of droplet evaporation is the third major finding of this work.

Note that the prevention of the diameter decrease by the nematodes and the associated accelerated decrease in the contact angle means that the critical contact angle θ_c will be reached sooner. This means that the collective motion of the nematodes in an evaporating droplet is a self-enhancing

process. The metachronal wave will accelerate the decrease in the contact angle, which in turn will make the metachronal wave even stronger as seen in the previous part of the article.

Force produced by the nematodes

To explain the existence of the transition angle θ_t, let us go back to the physics of droplets evaporation. The balance between the different forces acting on a droplet in contact with a flat solid surface is given by the Young's relation

$$\gamma_{sg} = \gamma_{sl} + \gamma_{lg}\cos\theta. \quad (1)$$

Here γ_{sg}, γ_{sl}, γ_{lg} are the surface tensions of solid/gas, solid/liquid and liquid/gas interfaces and θ is the contact angle as explained in the inset of Fig. 5. In simple words, γ_{lg} measures how much the liquid and ambient air molecules repel one another; γ_{sl} how much the liquid molecules repel the solid ones; and γ_{sg} how much the solid molecules repel the surrounding gas. Therefore, γ_{lg} and γ_{sl} tend to decrease the diameter of the droplet (assuming $\theta < 90°$), while γ_{sg} tend to increase it. In addition to these forces, the nematodes could exert and outward horizontal force γ_n on the boundary. We modify Young's relation to include this force per unit length giving

$$\gamma_{sg} + \gamma_n = \gamma_{sl} + \gamma_{lg}\cos\theta. \quad (2)$$

Note that as the angle θ will decrease, the horizontal force on the contact point coming from the surface tension contribution γ_{lg} will become stronger. Thus at some critical angle, the force from the nematodes γ_n would not be able any longer to oppose the surface tension force, and the mode of evaporation will change from that at constant diameter to the one at a constant contact angle. To verify this hypothesis let us assume that the force exerted by the nematodes is proportional to the density of the nematodes at the border $\gamma_n = F_n d_b$, where F_n is the force exerted by an individual nematode and d_b the density of nematodes at the border that we have previously measured. Our Young's relation at the transition angle then becomes

$$F_n d_b = \gamma_{sl} - \gamma_{sg} + \gamma_{lg}\cos\theta_t. \quad (3)$$

The three values of the transition angle in Fig. 4(a) are $\theta_t(25\%) = 63° \pm 0.15$, $\theta_t(50\%) = 56° \pm 0.25$ and $\theta_t(100\%) = 53° \pm 0.27$. The densities at the border for the two smallest density droplets can be directly taken from Fig. 2(c) with $d_b(25\%) = 9 \pm 0.5$ n mm^{-1} and $d_b(50\%) = 16 \pm 0.7$ n mm^{-1}. While we have not directly measured the border density of droplets at such a high concentration as of our 100% droplet, we can reasonably assume that because of the final possible packing, this density will be approximately the same that the one that we measured for our highest concentration droplet on Fig. 2c. By linearly interpolating between two points, we therefore obtain $d_b(100\%) = 19 \pm 1.1$ n mm^{-1}. Plotting d_b *versus* $\cos\theta_t$ we obtain a perfect straight line as predicted by our theory (Fig. 5).

The value of $\gamma_{lg} = 72.59(0.36)$ μN mm^{-1} [41] for water in contact with air at 21 °C temperature is well known and allows us to extract from the fit the force exerted by an individual nematode on the border $F_n = 1.08(0.11)$ μN. This in turn allow us to compute $\gamma_{sl} - \gamma_{sg} = 19.9(5.0)$ μN mm^{-1}. While we do not know exactly the composition of the PDMS coating that we used, the numerically and experimentally estimated values at room temperature of different varieties of PDMS in contact with vapor are $\gamma_{sg} \approx$ 20–23 μN mm^{-1} and PDMS in contact with water $\gamma_{sl} \approx$ 40–42 μN mm^{-1}.[42] This gives $\gamma_{sl} - \gamma_{sg} \approx$ 17–22 μN mm^{-1}, in excellent agreement with our measurements, which further validate our theory and hypothesis.

Note, that one can argue that eqn (3) should hold everywhere above the transition contact angle, as no droplet diameter change is observed in this region. However, the simplified eqn (3) does not take into account the pinning force acting on the contact line.[43] Nevertheless, in the regime that we are studying, the droplet diameter has already started to move and the pinning force is negligible. This is proven by the fact that we find the value of $\gamma_{sl} - \gamma_{sg}$, equivalent to the one in previous experiments, which indicate that an additional term for the pinning force is not needed.

Contrary to the nematodes in water, no transition to a constant contact angle evaporation can be observed on Fig. 2(a) for the nematodes in the growth solution. Indeed, the surface tension of a mixture of acetic acid and water at 5% concentration and 21 °C temperature is $\gamma_{vinegar} = 51.8(0.5)$ μN mm^{-1},[44] smaller than that of water. This alone would have changed the transition angles above to $\theta_t(25\%) = 55.1°$, $\theta_t(50\%) = 44.1°$ and $\theta_t(100\%) = 38.7°$. Additionally, the suspended particles in the growth medium should further oppose the reduction of the droplet diameter by contact line pinning.[45] Both of this reasons explain, why a transition to a different mode of evaporation is generally not observed for droplets of the initial growth solution.

Is the measured force of approximately 1 μN per nematode reasonable? Forces where directly measured on the similarly sized *C. elegans* by observing the deviation of micropillars when

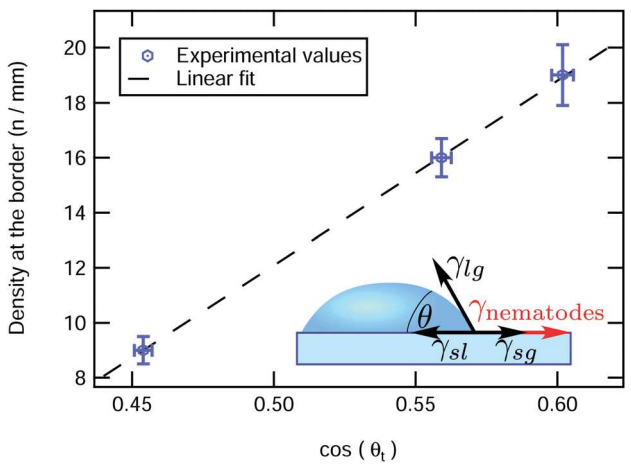

Fig. 5 Expected density at the border *versus* the cosine of the transition angle θ_t for the three droplets from Fig. 3 and 4. Inset: Diagram of forces acting on the contact point in a droplet residing on a flat surface.

pushed by the nematodes bodies and gave values in the range of 5 to 30 μN.[46] An almost order of magnitude difference can be explained by two considerations. First, the nematode is not oriented perfectly perpendicular to the surface, but at an angle of $\approx 20^\circ$, using a part of it's force to move along the wall. However, such a small angle will provide only a very small decrease in the force ($\cos(20) \approx 0.94$). Second, if one looks at Fig. 1(d), we can see that only a small proportion of nematodes touch the border at a given time, which should further reduce the average force exerted over time. Finally, we expect that the force associated with forward motion that we measured, is only a small fraction of that exerted by the entire nematode on the fluid when swimming. Indeed, we have seen in the first part of the manuscript, that the motion of the nematodes is capable of deforming the droplet surface. Such deformation is directly proportional to the force exerted by the undulating nematode body on the droplet surface. The force needed to produce this curvature of the surface can be easily computed as described in the SV (ESI†), and give an estimated value of $F_{\text{undulation}} = 11$ μN, in good agreement with the forces produced by *C. elegans*.

Note, that such a good accuracy of the hypothesis that the force exerted by the nematodes is proportional to their density is actually surprising. We would expect that due to hydrodynamic interactions between the closely spaced nematodes, the force that they produce will depend on the spacing between them. Indeed, the measurement of produced flow, both in experiments on artificial cilia[47] and simulations of straight paddles moving with metachronal wave motion,[48] shows that it depend on the spacing between the beating organisms. The border density of $d_b \approx 10$–20 n mm^{-1} lead to a spacing between the nematodes of $s_n \approx 0.05$–0.1 mm. Given the typical length of the nematodes is $L_n \approx 1$ mm, this provide a relative spacing of $s_n/L_n \approx 0.05$–1, at which we would expect a noticeable decrease in efficiency with the reduction of spacing according to the simulations of straight paddlers[48] (assuming Re = 0.4 as explained in the next section). However, the applicability of a simplistic model of straight paddles to the much more complex shape of nematodes is questionable.

Discussion and conclusions

We have studied the collective motion of the nematode *T. aceti* inside droplets deposited on a flat surface. We have shown that if the concentration of eels is high enough, a metachronal wave will form on the edge when the contact angle of the droplet is below a critical value of $\theta_c = 68.5^\circ$. This collective state is an experimental illustration of *swarmalators*, particles that at the same time align their motion and their oscillations. We propose that the dependence of the collective wave on the contact angle of the drop is due to the increased probability of interactions between the nematodes bodies at low contact angle. The number of nematodes participating in the metachronal wave increase as the contact angle of the drop decreases, which can be explained by the fact that synchronization will increase the free space available at the border. We also show that the collective motion of the nematodes can change the physics of drop evaporation. Initial evaporation of droplets containing synchronously moving nematodes occurs mostly at constant diameter rather than at constant contact angle. This allows us to estimate the magnitude of the force exerted by self propulsion of the nematode on the border at $F_n = 1.08$ μN. This is the force of interest for possible use of nematodes for displacing objects. Conversely, the force produced by the undulation of the nematodes bodies can be estimated from the deformation of the drop surface and is $F_{\text{undulation}} = 11$ μN, in good agreement with direct measurements of the force produced by the specie *C. elegans*.

Another novelty of our system stems from the relatively large length of our nematodes, $L_n \sim 1$ mm, which combined with a typical swim velocity $v_{swim} \approx 0.4$ mm s^{-1} [17] leads to a characteristic Reynolds number of Re = 0.4. This places our system in the intermediate Reynolds number regime[49] in contrast to the low Reynolds number regime in which most microorganisms, which exhibit collective or synchronous motion, reside.[50–53] This means that the inertia in the motion of the nematodes cannot be neglected. The full Navier–Stokes equations should be used to describe such systems, which become non-linear and time dependent, and thus can lead to many interesting new states.[54]

To better understand what drives the formation of the collective state it could be interesting to be able to genetically choose the properties of the nematodes such as sensitivity to light or touch, in the same way as it is done for the much more studied *C. elegans*. While it is in theory possible to apply the same genetic toolkit to *T. aceti*, this will certainly be a major undertaking. For this reason, we tried to reproduce the collective states of *T. aceti* in suspensions of *C. elegans*. However, as described in part VI (ESI†), we were unable to observe any synchronization of oscillations of *C. elegans* for the various densities and droplet shapes that we tried. This absence of synchronization may be explained by the shorter bodies of *C. elegans*.

We believe that *T. aceti* is an extremely promising organism both for exploring the behavior of *swarmalators* and the states of active matter at intermediate Reynolds numbers. Much of the physics of this nematode remains to be explored; the nature of the phase transition to collective motion, the formation of clusters, its behavior in liquids of different viscosity or inside confined spaces. Given that the theoretical exploration of the motion of the nematode will require the study of the full Navier–Stokes equations, this could lead to new developments in numerical and theoretical approaches. As we have shown in this article, the collective motion of the nematode produces strong fluid flows. As we have an external control parameter for the collective motion, in the form of the contact angle, we may in the future produce on-demand flows using specially designed channels. *T. aceti* combine ease of culture and experimentation with extremely interesting physics. We hope that this article will start a new thriving direction of research in the field of active matter.

Data accessibility

The original data for this manuscript is available at ref. 29.

Author contributions

A. P. designed the experiments and drafted the manuscript. A. P. and S. M. performed the experiments and analyzed the data. A. P. ad A. Q. conceived the study, performed analytical computations and edited the manuscript. All authors discussed the results and gave final approval for publication.

Funding

This work was supported by NASA grants 80NSSC17K0771 and 80NSSC21K0143; and National Science Foundation grants No. PHY-1757062 and No. DMR-1809318.

Conflicts of interest

The authors have no competing interests to declare.

Acknowledgements

We thank Myron W. Culver for giving us access to a wet lab. We thank William Houlihan for lending us an inverted microscope. We thank Nick Reilly for help procuring a centrifuge. We thank Doug Portman for helpful discussions on *C. elegans*. We thank Keith Nehrke, Sanjib K. Guha, Yunki Im and other members of Nehrke's lab for helping us explore *C. elegans*, and giving us materials and starting cultures to study *C. elegans*. We thank Steve Teitel and Hugues Chaté for their careful reading and critique of the earlier versions of this manuscript. We thank Sanjib K. Guha, Keith Nehrke and Randal C. Nelson for helpful suggestions and discussions.

References

1 M. C. Marchetti, J. F. Joanny, S. Ramaswamy, T. B. Liverpool, J. Prost and M. Rao, *et al.*, Hydrodynamics of soft active matter, *Rev. Mod. Phys.*, 2013, **85**(3), 1143–1189.
2 A. Sokolov, R. E. Goldstein, F. I. Feldchtein and I. S. Aranson, Enhanced mixing and spatial instability in concentrated bacterial suspensions, *Phys. Rev. E: Stat. Phys., Plasmas, Fluids, Relat. Interdiscip. Top.*, 2009, **80**(3), 031903.
3 M. Ballerini, N. Cabibbo, R. Candelier, A. Cavagna, E. Cisbani and I. Giardina, *et al.*, Interaction ruling animal collective behavior depends on topological rather than metric distance: Evidence from a field study, *Proc. Natl. Acad. Sci. U. S. A.*, 2008, **105**(4), 1232–1237.
4 D. S. Calovi, U. Lopez, S. Ngo, C. Sire, H. Chaté and G. Theraulaz, Swarming, schooling, milling: phase diagram of a data-driven fish school model, *New J. Phys.*, 2014, **16**(1), 015026.
5 J. Buck and E. Buck, Biology of Synchronous Flashing of Fireflies, *Nature*, 1966, **211**(5049), 562–564.
6 S. H. Strogatz, D. M. Abrams, A. McRobie, B. Eckhardt and E. Ott, Crowd synchrony on the Millennium Bridge, *Nature*, 2005, **438**(7064), 43–44.
7 G. I. Taylor, Analysis of the swimming of microscopic organisms, *Proc. R. Soc. London, Ser. A*, 1951, **209**(1099), 447–461.
8 T. Niedermayer, B. Eckhardt and P. Lenz, Synchronization, phase locking, and metachronal wave formation in ciliary chains. Chaos: An Interdisciplinary, *J. Nonlinear Sci.*, 2008, **18**(3), 037128.
9 D. R. Brumley, M. Polin, T. J. Pedley and R. E. Goldstein, Hydrodynamic Synchronization and Metachronal Waves on the Surface of the Colonial Alga Volvox carteri, *Phys. Rev. Lett.*, 2012, **109**, 268102.
10 J. Elgeti and G. Gompper, Emergence of metachronal waves in cilia arrays, *Proc. Natl. Acad. Sci. U. S. A.*, 2013, **110**(12), 4470–4475.
11 K. P. O'Keeffe, H. Hong and S. H. Strogatz, Oscillators that sync and swarm, *Nat. Commun.*, 2017, **8**(1), 1504.
12 N. Kruk, Y. Maistrenko and H. Koeppl, Self-propelled chimeras, *Phys. Rev. E*, 2018, **98**, 032219.
13 D. Levis, I. Pagonabarraga and B. Liebchen, Activity induced synchronization: Mutual flocking and chiral self-sorting, *Phys. Rev. Res.*, 2019, **1**, 023026.
14 F. Jimenez-Morales, Oscillatory behavior in a system of swarmalators with a short-range repulsive interaction, *Phys. Rev. E*, 2020, **101**, 062202.
15 N. Kruk, J. A. Carrillo and H. Koeppl, Traveling bands, clouds, and vortices of chiral active matter, *Phys. Rev. E*, 2020, **102**, 022604.
16 R. K. Manna, O. E. Shklyaev and A. C. Balazs, Chemical pumps and flexible sheets spontaneously form self-regulating oscillators in solution, *Proc. Natl. Acad. Sci. U. S. A.*, 2021, **118**(12), e2022987118.
17 A. C. Quillen, A. Peshkov, E. Wright and S. McGaffigan, Metachronal waves in concentrations of swimming Turbatrix aceti nematodes and an oscillator chain model for their coordinated motions, *Phys. Rev. E*, 2021, **104**(1), 014412.
18 N. H. P. Nguyen, E. Jankowski and S. C. Glotzer, Thermal and athermal three-dimensional swarms of self-propelled particles, *Phys. Rev. E*, 2012, **86**, 011136.
19 Y. L. Chuang, T. Chou and M. R. D'Orsogna, Swarming in viscous fluids: Three-dimensional patterns in swimmer- and force-induced flows, *Phys. Rev. E*, 2016, **93**, 043112.
20 J. P. Hernandez-Ortiz, C. G. Stoltz and M. D. Graham, Transport and collective dynamics in suspensions of confined swimming particles, *Phys. Rev. Lett.*, 2005, **95**, 204501.
21 A. Bricard, J. B. Caussin, D. Das, C. Savoie, V. Chikkadi and K. Shitara, *et al.*, Emergent vortices in populations of colloidal rollers, *Nat. Commun.*, 2015, **6**, 7470.
22 E. Lushi, H. Wioland and R. E. Goldstein, Fluid flows created by swimming bacteria drive self-organization in confined suspensions, *Proc. Natl. Acad. Sci. U. S. A.*, 2014, **111**(27), 9733–9738.
23 A. C. Quillen, J. P. Smucker and A. Peshkov, Boids in a loop: Self-propelled particles within a flexible boundary, *Phys. Rev. E*, 2020, **101**, 052618.
24 A. Sokolov, M. M. Apodaca, B. A. Grzybowski and I. S. Aranson, Swimming bacteria power microscopic gears, *Proc. Natl. Acad. Sci. U. S. A.*, 2010, **107**(3), 969–974.

25 R. Di Leonardo, L. Angelani, D. Dell'Arciprete, G. Ruocco, V. Iebba and S. Schippa, *et al.*, Bacterial ratchet motors, *Proc. Natl. Acad. Sci. U. S. A.*, 2010, **107**(21), 9541–9545.
26 G. Vizsnyiczai, G. Frangipane, C. Maggi, F. Saglimbeni, S. Bianchi and R. Di Leonardo, Light controlled 3D micromotors powered by bacteria, *Nat. Commun.*, 2017, **8**(1), 15974.
27 Z. Gao, H. Li, X. Chen and H. P. Zhang, Using confined bacteria as building blocks to generate fluid flow, *Lab Chip*, 2015, **15**(24), 4555–4562.
28 T. Masuda, A. M. Akimoto, K. Nagase, T. Okano and R. Yoshida, Artificial cilia as autonomous nanoactuators: design of a gradient self-oscillating polymer brush with controlled unidirectional motion, *Sci. Adv.*, 2016, **2**(8), e1600902.
29 A. Peshkov, S. McGaffigan and A. Quillen, Supplemental material for the article: Synchronized oscillations in swarms of nematode Turbatrix aceti, https://doiorg/106084/m9fig sharec5476659. 2021.
30 J. Yuan, D. M. Raizen and H. H. Bau, A hydrodynamic mechanism for attraction of undulatory microswimmers to surfaces (bordertaxis), *J. R. Soc., Interface*, 2015, **12**, 20150227.
31 B. Vincenti, G. Ramos, M. L. Cordero, C. Douarche, R. Soto and E. Clement, Magnetotactic bacteria in a droplet self-assemble into a rotary motor, *Nat. Commun.*, 2019, **10**(1), 5082.
32 E. Demir, Y. I. Yaman, M. Basaran and A. Kocabas, Dynamics of pattern formation and emergence of swarming in Caenorhabditis elegans, *eLife*, 2020, **9**, e52781 C1 eLife 2.
33 A. Deblais, A. Maggs, D. Bonn and S. Woutersen, Phase Separation by Entanglement of Active Polymerlike Worms, *PRL*, 2020, **124**(20), 208006.
34 Y. Ozkan-Aydin, D. I. Goldman and M. S. Bhamla, Collective dynamics in entangled worm and robot blobs, *Proc. Natl. Acad. Sci. U. S. A.*, 2021, **118**(6), e2010542118.
35 M. R. Bittermann, D. Bonn, S. Woutersen and A. Deblais, Light-switchable deposits from evaporating drops containing motile microalgae, *Soft Matter*, 2021, **17**(27), 6536–6541.
36 H. Hu and R. G. Larson, Evaporation of a Sessile Droplet on a Substrate, *J. Phys. Chem. B*, 2002, **106**(6), 1334–1344, DOI: 10.1021/jp0118322.
37 C. Bourges-Monnier and M. Shanahan, Influence of evaporation on contact angle, *Langmuir*, 1995, **11**(7), 2820–2829.
38 R. G. Picknett and R. Bexon, The evaporation of sessile or pendant drops in still air, *J. Colloid Interface Sci.*, 1977, **61**(2), 336–350.
39 K. S. Birdi and D. T. Vu, Wettability and the evaporation rates of fluids from solid surfaces, *J. Adhes. Sci. Technol.*, 1993, **7**(6), 485–493, DOI: 10.1163/156856193X00808.
40 M. J. Kisiel, J. M. Castillo, L. S. Zuckerman, B. M. Zuckerman and S. Himmelhoch, Studies on ageing in Turbatrix aceti, *Mech. Ageing Dev.*, 1975, **4**, 81–88.
41 N. B. Vargaftik, B. N. Volkov and L. D. Voljak, International Tables of the Surface Tension of Water, *J. Phys. Chem. Ref. Data*, 1983, **12**(3), 817–820, DOI: 10.1063/1.555688.
42 A. E. Ismail, G. S. Grest, D. R. Heine, M. J. Stevens and M. Tsige, Interfacial Structure and Dynamics of Siloxane Systems: PDMS-Vapor and PDMS-Water, *Macromolecules*, 2009, **42**(8), 3186–3194, DOI: 10.1021/ma802805y.
43 R. Tadmor, Open Problems in Wetting Phenomena: Pinning Retention Forces, *Langmuir*, 2021, **37**(21), 6357–6372, DOI: 10.1021/acs.langmuir.0c02768.
44 E. Alvarez, G. Vazquez, M. Sanchez-Vilas, B. Sanjurjo and J. M. Navaza, Surface Tension of Organic Acids + Water Binary Mixtures from 20 °C to 50 °C, *J. Chem. Eng. Data*, 1997, **42**(5), 957–960, DOI: 10.1021/je970025m.
45 F. Parisse and C. Allain, Shape changes of colloidal suspension droplets during drying, *J. Phys. II*, 1996, **6**(7), 1111–1119.
46 A. Ghanbari, V. Nock, W. Wang, R. Blaikie, J. G. Chase and X. Chen, *et al.* Force Pattern Characterization of C. elegans in Motion, In 2008 15th International Conference on Mechatronics and Machine Vision in Practice, ed. anonymous, 2008. p. 634–639.
47 D. Xiaoguang, L. G. Zhan, H. Wenqi, Z. Rongjing, R. Ziyu and R. Op, *et al.*, Bioinspired cilia arrays with programmable nonreciprocal motion and metachronal coordination, *Sci. Adv.*, 2020, **6**(45), 9323, DOI: 10.1126/sciadv.abc9323.
48 S. Granzier-Nakajima, R. D. Guy and C. Zhang-Molina, A Numerical Study of Metachronal Propulsion at Low to Intermediate Reynolds Numbers, *Fluids*, 2020, **5**(2), 86.
49 D. Klotsa, As above, so below, and also in between: mesoscale active matter in fluids, *Soft Matter*, 2019, **15**(44), 8946–8950.
50 E. M. Purcell, Life at low Reynolds number, *Am. J. Phys.*, 1977, **45**(1), 3–11, DOI: 10.1119/1.10903.
51 S. Gueron and K. Levit-Gurevich, Computation of the Internal Forces in Cilia: Application to Ciliary Motion, the Effects of Viscosity, and Cilia Interactions, *Biophys. J.*, 1998, **74**(4), 1658–1676.
52 A. Vilfan and F. Jülicher, Hydrodynamic Flow Patterns and Synchronization of Beating Cilia, *Phys. Rev. Lett.*, 2006, **96**(5), 058102.
53 N. Uchida and R. Golestanian, Generic Conditions for Hydrodynamic Synchronization, *Phys. Rev. Lett.*, 2011, **106**, 058104.
54 R. Chatterjee, N. Rana, R. A. Simha, P. Perlekar and S. Ramaswamy Fluid flocks with inertia, 2019, arXiv preprint arXiv:190703492.

